

Nanoscale depth profiling of residual stresses due to fine surface finishing

Joris Everaerts, Enrico Salvati, Alexander M. Korsunsky

Dr. J. Everaerts

Department of Engineering Science, University of Oxford, Oxford OX1 3PJ, UK

Current affiliation: Mechanical Metallurgy Laboratory, École Polytechnique Fédérale de Lausanne, Station 12, CH-1015 Lausanne, Switzerland

E-mail: joris.everaerts@epfl.ch

Abstract

Mechanical polishing is commonly used for both surface finishing and metallographic sample preparation for a broad range of materials. However, polishing causes local deformation and induces residual stress, which has an important effect on many surface phenomena. Until recently, it has not been possible to quantify the nanoscale depth variation of polishing-induced plastic deformation (eigenstrain) and the associated residual stress. In this study, the magnitude and depth of polishing-induced residual stress are evaluated directly for the first time, by focused ion beam milling and digital image correlation using a micro-ring-core geometry (FIB-DIC method). Depth-resolved residual stress profiles are obtained with submicron resolution at the surface of a titanium alloy sample that was subjected to various polishing steps. It is found that electrochemical polishing and polishing with colloidal silica does not induce any significant residual stress. However, polishing with diamond slurry leads to the formation of compressive residual stresses of up to 300 MPa, which extend deeper into the material when larger diamond particles are used. This study paves the way for further research on polishing and its effect on surface properties.

Keywords: polishing, residual stress, FIB-DIC, titanium, eigenstrain

Main text

Mechanical polishing has been used as a finishing process for metals for many centuries in order to obtain smooth, mirror-like surfaces with minimal roughness. As a sample preparation method for metallographic studies, polishing can be attributed to Henry Clifton Sorby's work during the late 19th century, and it is now common practice in all materials science laboratories. This method involves pressing the sample being finished onto a rotating polishing cloth that is covered with a slurry of hard abrasive particles, most commonly made of diamond. In order to obtain a sufficiently smooth surface finish, polishing is generally performed in steps involving successively finer particles. The final step for ductile metals often consists of colloidal silica polishing, with near-spherical soft particles of size in the order of 40 nm.^[1]

Surprisingly, the mechanism by which material is removed during polishing has been a matter of some debate. The notion that polishing simply removes material by abrasion, which was put forward by Hooke,^[2] was disputed by Beilby,^[3] who proposed that plastic surface flow and material redistribution led to smoothening. This theory was supported by electron diffraction measurements on polished surfaces, which pointed out the presence of a thin amorphous layer of up to 50 nm, later dubbed the 'Beilby layer'.^[4-6] Moreover, experiments on non-oriented polycrystalline copper and gold showed that after polishing another layer of up to 1 μm was formed underneath this amorphous surface layer, which consisted of crystals that assumed a preferential orientation due to compressive loads.^[7] More recent experiments provide indications of plastic flow on a polished titanium surface, but without evidence for amorphisation.^[8] Transmission electron microscopy examinations of polished copper also showed plastic deformation, without the presence of an amorphous layer.^[9] It is therefore believed that with modern polishing methods the removal mechanism is abrasion, which does cause plastic deformation but does not introduce any discernible amorphisation of the surface layer.^[1]

In any case, it is clear that mechanical polishing modifies the surface structure of the material due to plastic deformation. This can result in microstructural changes, e.g. shear bands and grain refinement, and more generally causes the formation of a strained region. The depth of this deformed layer in the case of brass has been examined by transmission electron microscopy and found to be respectively 1 and 0.7 μm after polishing with 6 and 1 μm diamond particles.^[1] However, research on this topic is limited, and there is a lack of quantitative information regarding the magnitude of plastic strain that is induced by polishing. Furthermore, a region of plastic strain would give rise to a residual stress field that may extend deeper into the material. The presence of polishing-induced residual stresses has been shown to affect, for example, the ageing sensitivity of zirconia.^[10] Near-surface residual stresses are also known to have a significant influence on the initiation of fatigue cracks and thus fatigue life of components.^[11-13] Additionally, polishing can affect the results of surface-sensitive measurements such as nanoindentation^[14] and electron backscatter diffraction.^[15]

The lack of data on polishing-induced residual stresses can be attributed to the fact that it is challenging to measure near-surface residual stress at such a fine scale. However, recent developments in the ring-core ‘focused ion beam – digital image correlation’ (FIB-DIC) technique have opened up the possibility to obtain depth-resolved residual stress information with submicron resolution.^[16,17] This method utilises a FIB to perform an incremental milling of a circular trench, as shown in **Figure 1**, thereby creating a cylindrical micropillar that is gradually being relieved from residual stress.^[18] By patterning the top surface of this micropillar with a thin sputtered Au coating (or otherwise to create contrast), the strain relief of the pillar can be determined after each incremental milling step using DIC analysis of scanning electron microscopy (SEM) images. The change in strain relief is captured for increasing milling depths in a stepwise fashion, which means that information about in-depth residual stress variation is

acquired. By considering the ring-core geometry and the strain relief after each milling step, the depth-resolved residual stress profile can be obtained using the non-integral method reported by Korsunsky et al.^[16]

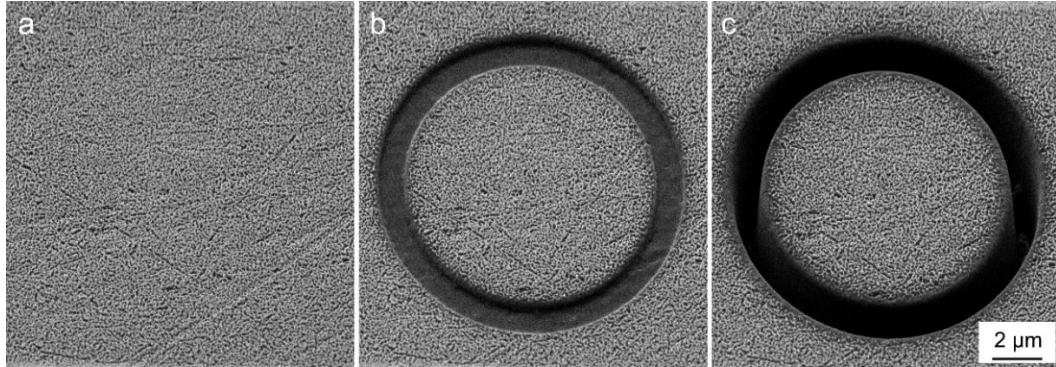


Figure 1. SEM images illustrating different stages of the ring-core FIB-DIC technique: (a) Surface patterning; (b) First incremental milling step; (c) Final milling step

In this study, the depth and magnitude of residual stresses induced by mechanical polishing is evaluated directly for the first time, by applying the ring-core FIB-DIC technique to a titanium alloy sample after various polishing steps. The microstructure of the sample, shown in **Figure 2**, consists of a typical α - β structure, with the α grain size approximately 1 μm . The grain size is important because the ring-core FIB-DIC technique becomes sensitive to inter- and intragranular (Type II+III) residual stresses if the micropillar diameter is in the order of the grain size.^[19] Therefore, a small grain size is advantageous for the current study, because ring-core FIB-DIC measurements with small micropillar diameters are needed to achieve the necessary sensitivity to residual stresses at a small scale. In this case, the smallest ring-core measurements, i.e. with diameter 5 μm , contain multiple grains and should thus have limited scatter as a result of Type II+III residual stresses. This allows for evaluating only the grain-average (Type I) residual stresses that are induced by polishing.

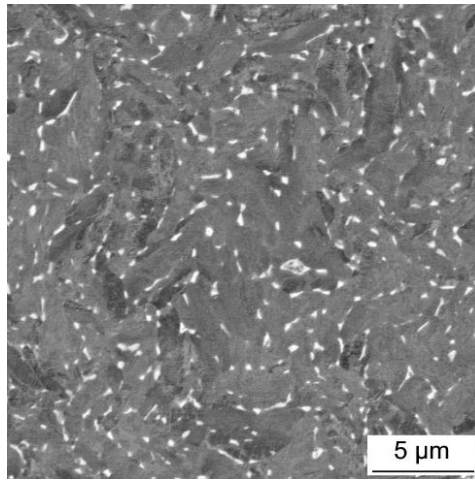


Figure 2. Backscattered electron image of Ti-6Al-4V sample surface after electrochemical polishing

Figure 3 shows the average in-plane residual stress profiles as a function of depth that are present in the material after the various polishing steps. The error bars represent the standard deviations between different ring-core FIB-DIC measurements. It can be observed that in the electropolished state the material does not contain any significant surface residual stress, which confirms the absence of any remaining intrinsic Type I residual stresses in the material. Furthermore, there is no noticeable change after colloidal silica polishing, suggesting that it did not induce any discernible residual stress. However, after polishing with 0.25 μm diamond slurry a compressive stress of approximately 50 MPa is present near the surface, reducing to ~0 MPa at a depth of circa 0.8 μm. Polishing with 1 μm diamond slurry induces a near-surface residual stress of up to 300 MPa in compression, which decreases to ~0 MPa at a depth of roughly 1.3 μm. After polishing with 3 μm diamond slurry, the maximum value of compressive

residual stress near the surface remains within the same order of magnitude, but only reduces to ~0 MPa at a larger depth of approximately 3.5 μm .

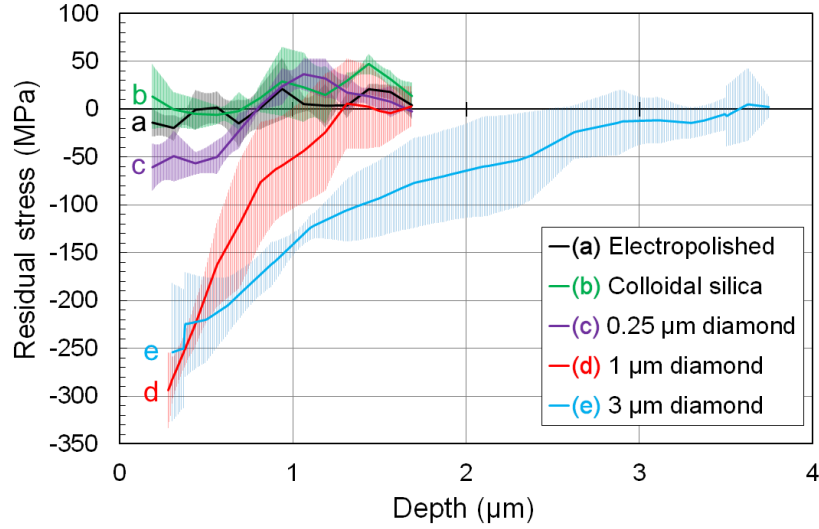


Figure 3. In-plane residual stress as a function of depth after various polishing steps (error bars represent standard deviation)

The residual stress profiles can be analysed further by use of the eigenstrain theory.^[20] This approach allows quantifying the amount of plastic deformation introduced by polishing. Eigenstrain refers to inelastic strain that is stored in the material due to plasticity or other inelastic deformation mechanisms. The total compatible material strain ϵ_{total} can be decomposed into the sum of eigenstrain distribution ϵ^* and residual elastic strain distribution ϵ_{res} , so $\epsilon_{total} = \epsilon^* + \epsilon_{res}$. In the current case, the eigenstrain distribution is assumed to be equi-biaxial, as there is no preferential polishing direction. Taking x and y as two in-plane directions:

$$\epsilon_{xx}^* = \epsilon_{yy}^* = \epsilon^* \quad (1)$$

Close to the sample surface, the out-of-plane residual stress is assumed to be zero. Given that the total compatible strain in a thin layer on bulk substrate must be zero ($\epsilon_{total} = 0$), the eigenstrain distribution ϵ^* can be obtained via Hooke's law for plane stress as:

$$\epsilon^* = -\epsilon_{res} = -\frac{1-\nu}{E} \sigma_{res} \quad (2)$$

In this equation, σ_{res} represents the in-plane residual stress distribution, E is Young's modulus and ν is Poisson's ratio. **Figure 4** shows the eigenstrain distributions as a function of depth after various polishing steps. The amount of plastic deformation can now be evaluated by least-squares fitting of the following exponential curve:

$$\varepsilon^* = \varepsilon_{max}^* e^{-\frac{d}{d_0}} \quad (3)$$

In this equation, d represents the depth, and ε_{max}^* and d_0 are curve fitting parameters representing the maximum eigenstrain and the attenuation depth, respectively. From this analysis, ε_{max}^* and d_0 are found to be 3.67×10^{-3} and $0.41 \mu\text{m}$ after polishing with $1 \mu\text{m}$ diamond slurry, and 2.21×10^{-3} and $1.11 \mu\text{m}$ after polishing with $3 \mu\text{m}$ diamond slurry, respectively. Thus, the attenuation depth due to polishing d_0 and particle diameter D are found to be related as $d_0 \approx 0.4D$. On the other hand, the relation between ε_{max}^* and D appears to be more complex, and possibly depends on several polishing conditions, namely, applied pressure, properties of polishing cloth, etc. Because ε_{max}^* is a parameter that can be linked to the amount of plastic deformation, it would be worthwhile to further clarify this relation in future studies.

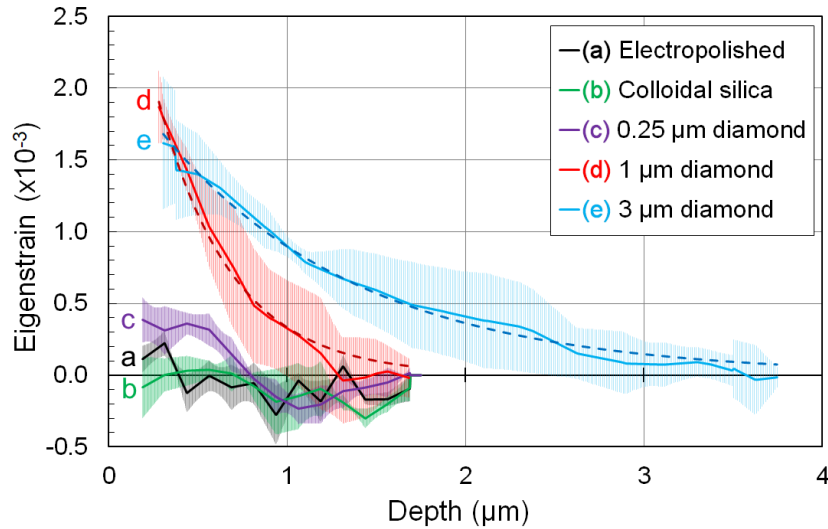


Figure 4. Eigenstrain distributions as a function of depth after various polishing steps, with exponential fitting (dashed lines)

Several interesting observations can be made regarding the obtained residual stress depth profiles. Firstly, the absence of residual stress after electrochemical polishing shows that the stress relief heat treatment was effective in removing any intrinsic Type I residual stresses that may have been present in the sample, for example due to its thermomechanical history. Secondly, polishing with colloidal silica did not induce any detectable changes in residual stress, not even at a depth of about 200 nm. There are a few possible explanations for this observation. The polishing mechanism is reported to be different for colloidal silica, and includes chemical interactions between the polishing fluid and the sample surface. It is suggested that this results in the continuous formation of a corrosion-inhibiting reaction layer, which is relatively brittle and therefore removed rather easily by the silica particles.^[1] This mechanism could therefore result in a surface that is virtually free of plastic deformation and, consequently, residual stress. On the other hand, the colloidal silica particles are in the 40 nm range, but the measurements in the current study do not reveal residual stresses that may be present at depths smaller than 200 nm. Additionally, these stresses may be too small to be measured with the ring-core FIB-DIC method. The sensitivity of this method could be increased by further reducing the micropillar diameter from 5 μm to 1 μm , for example. However, this would be in the order of the grain size of the material, which could lead to additional scatter due to Type II+III residual stresses.^[19]

The results after polishing with diamond slurry show a clear trend, in which larger diamond particles result in compressive residual stress that extends to increasingly larger depths. The depth of the compressed layer after polishing with 1 μm diamond slurry is roughly 1.3 μm , which is slightly larger than the reported depth of the plastically deformed layer in brass (0.7 μm) after polishing with a similar solution.^[1] This is plausible, given the fact that a layer of plastic strain would cause a self-equilibrated stress field that penetrates further into the surface, although caution should be exercised when comparing two different materials. Another interesting observation is that the maximum value of residual stress is found to be similar for

the 1 and 3 μm diamond polished surface. This would suggest that, at least for the current case of diamond-polished Ti-6Al-4V, there is a limit to the maximum value of residual stress that can be induced by mechanical polishing. This value may be governed by inherent material properties such as yield strength and plastic hardening. On the other hand, it may also be affected by the type of polishing cloth, because a synthetic fabric cloth was used for both the 1 and 3 μm diamond polishing steps, whereas a woven wool cloth was used for the 0.25 μm diamond polishing. A softer or more compliant cloth could reduce the local force exerted by the abrasive particles.^[21] Finally, in this study a reversed polishing scheme, i.e. with sequentially increasing particle sizes, was employed to avoid a significant influence of previous polishing steps. It is clear that if a regular scheme, i.e. with sequentially decreasing particle sizes, would be used, a deformation-free surface could only be obtained if the layer affected by the previous step was completely removed. This defines the required duration of each polishing step, which should be used as a guideline if a deformation-free surface is needed, e.g. for surface-sensitive measurements.

The current results illustrate that ring-core FIB-DIC milling can be successfully used to measure the depth and magnitude of polishing-induced residual stresses. Therefore, answers can now be sought to numerous questions regarding mechanical polishing. This includes, but is not limited to, the effect of polishing on different types of materials, the effect of polishing parameters such as speed, force, time, directionality, cloth type, type of abrasive particles, particle order sequence etc., the effect of the material's microstructure, as well as possible grain orientation effects, which can be measured by ring-core FIB-DIC inside individual grains.^[22] This knowledge can be used to optimise polishing procedures, and it will improve our understanding of surface phenomena such as wear, fatigue crack initiation, corrosion etc. on polished surfaces.

In summary, the depth and magnitude of residual stresses induced by mechanical polishing have been evaluated directly for the first time using ring-core FIB-DIC experiments. With this technique, depth resolved residual stress profiles with submicron resolution were obtained for an annealed titanium alloy sample subjected to various polishing steps. The most important conclusions can be summarised as follows:

- Measurements on the electrochemically polished surface showed that stress relief annealing successfully removed any remaining intrinsic residual stresses of Type I.
- Manual polishing with colloidal silica did not induce any discernible residual stress.
- Manual polishing with diamond slurry led to the formation of compressive residual stresses, which extended deeper into the material when larger diamond particles were used. More specifically, the depth of the affected layer was around 0.8, 1.3 and 3.5 μm after polishing with diamond particle sizes of 0.25, 1 and 3 μm , respectively.
- A maximum residual stress value of approximately 300 MPa in compression was reached after both polishing with 1 μm and with 3 μm diamond slurry.
- Eigenstrain analysis shows that the eigenstrain attenuation depth due to polishing d_0 and abrasive particle diameter D are related as $d_0 \approx 0.4D$.

By being able to directly evaluate polishing-induced residual stresses, it is now possible to investigate a wide range of questions regarding this commonly used surface finishing and metallographic preparation technique.

Experimental Section

Material preparation

The material used for this study was grade 5 titanium alloy (Ti-6Al-4V) wire, which was straightened by applying 1% plastic strain in tension and then stress relieved for 1 hour at 600 °C. A piece of this wire was embedded in epoxy resin to facilitate polishing. In order to prevent the previous polishing step from having a significant effect on the next, a reversed polishing scheme was used. Therefore, the sample was first electrochemically polished for 5 minutes with a current density of 2 kA m⁻² in an electrolyte containing ethanol (700 ml), isopropanol (300 ml), aluminium chloride (60 g) and zinc chloride (250 g). In the second step, the sample was manually polished for 1 hour with colloidal silica (Struers OP-S NonDry) on porous neoprene cloth (Struers MD-Chem). Next, the sample was manually polished for 1 hour using 0.25 μm diamond slurry (Spectrographic VS Poly Diamond, Struers MD-Mol cloth). The fourth step involved polishing with 1 μm diamond slurry (Spectrographic VS Poly Diamond, Struers MD-Plus cloth), again for 1 hour. In the final step, the sample was polished for 1 hour using 3 μm diamond slurry (Spectrographic VS Poly Diamond, Struers MD-Plus cloth). The rotation speed of the cloths was set to 300 rpm for all polishing steps, and the sample was slowly moved in a circle to avoid creating a preferential polishing direction.

Residual stress evaluation

In total, 18 ring-core FIB-DIC measurements were performed: three for the electrochemically polished sample (pillar diameters 5 μm), three for the colloidal silica polished sample (pillar diameters 5 μm), three for the 0.25 μm diamond polished sample (pillar diameters 5 μm), four for the 1 μm diamond polished sample (three with diameter 5 μm and one with diameter 10 μm) and five for the 3 μm diamond polished sample (three with diameter 10 μm and two with diameter 15 μm). The incremental FIB milling depth used for the ring-core experiments was 125, 200 and 250 nm for measurements with a pillar diameter of 5, 10 and 15 μm, respectively. The trench width of the milled ring was fixed at 1 μm. The measurements were performed at

random locations in the sample, and the distance between measurements as well as the distance from the nearest sample edge was at least five times the pillar diameter, as recommended by Lunt et al.^[23] All SEM imaging and FIB milling was done using a TESCAN LYRA3 dual beam microscope. Open source DIC code^[24] was used to obtain relief strain data. More specifically, five images were taken after each milling step using a pixel size of 8 nm. The displacements of the DIC markers, with 12 pixel grid spacing, were averaged over the five images per milling step, and subjected to the appropriate image drift correction and outlier removal procedures.^[25] The relief strain data were used to evaluate the in-plane residual stress profiles as a function of depth after the different polishing steps using the non-integral method for an equi-biaxial stress state described by Korsunsky et al.^[16,17] The sensitivity of this method extends to a depth of maximum 30% of the diameter of the micropillar (i.e. 1.5 μm for a 5 μm micropillar, 3 μm for a 10 μm micropillar etc.). For this reason, larger micropillar diameters were used when it was necessary to obtain information at larger depths. The Young's modulus and Poisson's ratio were taken as 110 GPa and 0.3, respectively.^[26] It should be noted that there were no significant differences in strain relief between different in-plane directions on the sample surface, indicating that there was no preferential polishing direction.

References

- [1] L. E. Samuels, *Metallographic Polishing by Mechanical Methods*, ASM International, **2003**.
- [2] R. Hooke, in *Micrographia*, The Royal Society, **1665**.
- [3] G. Beilby, *Aggregation and Flow of Solids: Being the Records of an Experimental Study of the Micro-Structure and Physical Properties of Solids in Various States of Aggregation*, Macmillan, London, **1921**.
- [4] G. I. Finch, A. G. Quarrell, *Nature* **1936**, *137*, 516.
- [5] R. C. French, G. P. Thomson, *Proceedings of the Royal Society of London. Series A, Containing Papers of a Mathematical and Physical Character* **1933**, *140*, 637.
- [6] T. Suratwala, W. Steele, L. Wong, M. D. Feit, P. E. Miller, R. Dylla-Spears, N. Shen, R. Desjardin, *Journal of the American Ceramic Society* **2015**, *98*, 2395.
- [7] C. S. Lees, E. K. Rideal, *Trans. Faraday Soc.* **1935**, *31*, 1102.
- [8] A. S. Iquebal, D. Sagapuram, S. Bukkapatnam, <http://arxiv.org/abs/1610.09719> **2016**.
- [9] D. M. Turley, L. E. Samuels, *Metallography* **1981**, *14*, 275.
- [10] S. Deville, J. Chevalier, L. Gremillard, *Biomaterials* **2006**, *27*, 2186.
- [11] L. Tan, D. Zhang, C. Yao, D. Wu, J. Zhang, *Journal of Manufacturing Processes* **2017**, *26*, 155.
- [12] R. M. N. Fleury, E. Salvati, D. Nowell, A. M. Korsunsky, F. Silva, Y. H. Tai, *International Journal of Fatigue* **2019**, *119*, 34.
- [13] G. E. Dieter, *Mechanical Metallurgy*, McGraw-Hill Book Company, New York, **1962**.
- [14] S. Pathak, D. Stojakovic, R. Doherty, S. R. Kalidindi, *Journal of Materials Research* **2009**, *24*, 1142.
- [15] J. Guo, S. Amira, P. Gougeon, X. G. Chen, *Materials Characterization* **2011**, *62*, 865.
- [16] A. M. Korsunsky, E. Salvati, A. G. J. Lunt, T. Sui, M. Z. Mughal, R. Daniel, J. Keckes, E. Bemporad, M. Sebastiani, *Materials and Design* **2018**, *145*, 55.

- [17] E. Salvati, L. Romano-Brandt, M. Z. Mughal, M. Sebastiani, A. M. Korsunsky, *Journal of the Mechanics and Physics of Solids* **2019**, *125*, 488.
- [18] A. M. Korsunsky, M. Sebastiani, E. Bemporad, *Materials Letters* **2009**, *63*, 1961.
- [19] J. Everaerts, X. Song, B. Nagarajan, A. M. Korsunsky, *Surface and Coatings Technology* **2018**, *349*, 719.
- [20] T. Mura, in *Micromechanics of Defects in Solids*, Springer Netherlands, Dordrecht, **1987**, pp. 1–73.
- [21] G. Petzow, *Metallographic Etching: Techniques for Metallography, Ceramography, Plastography*, ASM International, New York, **1999**.
- [22] J. Everaerts, E. Salvati, F. Uzun, L. Romano Brandt, H. Zhang, A. M. Korsunsky, *Acta Materialia* **2018**, *156*, 43.
- [23] A. J. G. Lunt, N. Baimpas, E. Salvati, I. P. Dolbnya, T. Sui, S. Ying, H. Zhang, A. K. Kleppe, J. Dluhoš, A. M. Korsunsky, *The Journal of Strain Analysis for Engineering Design* **2015**, *50*, 426.
- [24] M. Senn, “Digital Image Correlation and Tracking,” can be found under <https://uk.mathworks.com/matlabcentral/fileexchange/50994-digital-image-correlation-and-tracking>, **2016**.
- [25] A. J. G. Lunt, A. M. Korsunsky, *Surface and Coatings Technology* **2015**, *283*, 373.
- [26] G. Lütjering, J. C. Williams, *Titanium*, Springer-Verlag Berlin Heidelberg, **2007**.